

# Power Flow Numerical Assessment of a STATCOM iUPQC Utility Interface for Microgrids

M. Montagner<sub>1</sub>, C. Rech<sub>2</sub> and M. Mezaroba<sub>1</sub>

1 - Department of Electrical Engineering - Santa Catarina State University - Joinville - SC - Brazil

2 - Power Electronics and Control Research Group - Federal University of Santa Maria - Santa Maria - Brazil

e-mail: matheus.mtg60@gmail.com, cassiano.rech@gmail.com, marcello.mezaroba@udesc.br

**Abstract**— The dual unified power quality conditioner (iUPQC) is an active filter that has been studied to be applied as utility interface in microgrid applications. It regulates the voltage of the microgrid side and controls the power flow between the grid and microgrid side. Besides that, ancillary functions to grid side has been proposed to extend its power quality compensation. This paper presents a detailed analytical and numerical analysis of the power flow of an iUPQC, which operates as an utility interface in microgrid applications with the extended function of STATCOM. It can compensate not only the disturbances at the load or microgrid side but also provides a RMS voltage regulation at the Point of Common Coupling (PCC), thus, providing reactive power to the grid. Moreover, the iUPQC power flow is evaluated considering the implementation of the power angle control (PAC), a technique used to share and equalize the power processed by each converter allowing the optimization of this conditioner. Therefore, this study can support the understanding of the power flow of the iUPQC operating as STATCOM, in order to share and optimize the available power in the iUPQC converters using PAC.

**Keywords**—iUPQC, microgrids, STATCOM, Power Angle Control (PAC), Power flow analysis

## I. INTRODUCTION

The necessity of the reduction of carbon emissions has been motivating the growth of renewable electrical energy sources. Besides that, the electrical energy demand is always increasing. In this scenario, distributed energy resources based on renewable energy source and the microgrid concept has been proposed as a solution to have electrical energy generation with less environment impact [1] [2].

However, due to intermittence characteristic of renewable energy resources, microgrids topologies, control and operations strategies have been developed to ensure stable operation of microgrids [3].

In this sense, Utility Interfaces (UI) converters have been proposed for microgrid applications to make easier the controlling of the power system [4]-[6]. UI converter is connected between the grid and microgrid buses where the main function is controlling the power flow between the buses [4] [5]. It makes easier the control of the power system once the control of a group of loads and generation is centered in the UI converter. Besides that, it can be used to provide a regulated voltage in the microgrid side, improving the microgrid energy quality, and to provide ancillary functions to enhance the energy quality in the grid side [5] [7].

The iUPQC originally is an active power filter (APF) and it is composed of a series active filter (srAPF) and a shunt

active filter (shAPF) connected at the same DC bus in a back-to-back configuration. This configuration allows the conditioning of grid voltage and the load current simultaneously [8] [9].

For the reason of iUPQC features, it is a converter topology that can be used as UI in microgrids, controlling the power flow between the grid and microgrid side, regulating the microgrid bus voltage and compensating the microgrid load disturbances [10] [11].

Besides that, the STATCOM functionality can be implemented in the iUPQC regulating the RMS voltage at the PCC by providing reactive power to the grid side [12]. This functionality allows to optimize the use of the converter when there is available power to be processed in the converter, extending its functionalities and improving its viability. The operation of iUPQC as UI for microgrids and with the STATCOM functionality is called in this paper as multifunctional utility interface iUPQC (M-iUPQC).

In iUPQC, the srAPF compensates the grid voltage disturbances while shAPF needs to compensate the load current disturbances. It means that under normal operation, with the PCC voltage around 1.0 pu, the power processed by shAPF is quite bigger than srAPF [9]. This condition makes the srAPF underused once no power is processed, increases the conditioner losses and make difficult the modularization of the converters. This power unbalance issue of iUPQC is even more critical in an M-iUPQC because the shAPF needs to provide the reactive power to the microgrid and grid side while srAPF does not have power process [11].

To reduce the power unbalanced between the converters of iUPQC, in [12] and [13], the Power Angle Control (PAC) technique is presented. PAC consists of to impose a phase delay between the fundamental term of PCC voltage and load voltage in such a way the allow the power sharing between the converters of iUPQC. However, there is a lack of studies providing either numerical or experimental evaluation of PAC technique considering iUPQC operating as STATCOM either for this conditioner operating as active filter or as UI in microgrids applications.

Therefore, this paper presents an analytical and numerical analysis of the power flow in the M-iUPQC with the PAC applied. The contribution of current study resides on to provide a numerical assessment of the power flow in a M-iUPQC. In addition, it brings an evaluation the effectiveness of the PAC to share and balance the power processed by each converter of iUPQC by the equations developed and a PAC scheme proposed.

## II. iUPQC POWER FLOW ANALYSIS

The main objective of this analysis is to obtain equations that describe the power flow between the converters of the M-iUPQC in function of  $\theta$ , which is the angle displacement of fundamental term of PCC voltage ( $v_{1pc}$ ) and fundamental term of current ( $i_{1pc}$ ), and  $\delta$ , which is the angle displacement between microgrid voltage ( $v_{1ul}$ ) and  $v_{1pc}$ , as are shown in Fig. 1.

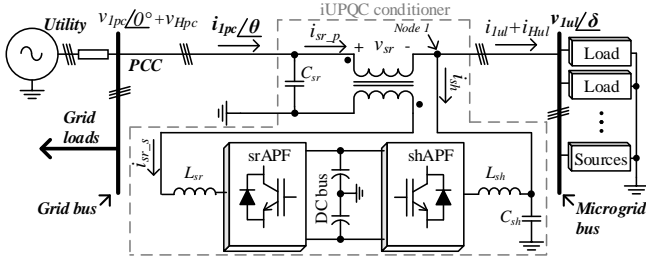


Fig. 1. Connection of a M-iUPQC between the grid and microgrid bus

### A. Features of M-iUPQC and simplifications used in this analysis

In a closed-loop controlled iUPQC, the shAPF operates as a controlled voltage source and it imposes the load voltage to be sinusoidal and in phase with the PCC voltage ( $v_{1pc}$ ). In contrast, the srAPF operates as a controlled current source and maintains the PCC current ( $i_{1pc}$ ) balanced, with low distortion and in phase with  $v_{1pc}$ . Moreover, iUPQC ideally does not have active power consumption and the amplitude of  $i_{1pc}$  is defined by the active power of the microgrid loads [9].

In MS-iUPQC, the amplitude of fundamental PCC voltage is regulated by controlling reactive power flow between the conditioner and the grid side. This is done by controlling the fundamental quadrature term amplitude of the PCC current ( $i_{1pc}$ ) [11]. The sum of the direct and quadrature components of the current in the PCC results in an equivalent current that has an angular displacement of  $\theta^\circ$  regarding to fundamental PCC voltage ( $v_{1pc}$ ). Consequently,  $i_{1pc}$  amplitude is not only defined by the loads active power of the microgrid loads as in the conventional iUPQC. Therefore, maintaining a constant microgrid load, larger displacement angles result in a higher reactive power support to the grid.

Finally, as previously stated, PAC technique consists of to impose a phase delay between microgrid and grid voltage. This phase displacement is represented by the  $\delta$  angle.

In addition, the power losses in the iUPQC as well as switching frequency harmonic components were ignored. Finally, the fundamental term of PCC voltage ( $v_{1pc}$ ) was defined as the reference voltage so that its phase angle is  $0^\circ$ .

To calculate the power flow of each converter, the concepts defined by IEEE 1459-2010 were adopted [14]. This standard has definitions for measuring electric power quantities that were used in this paper as reference to evaluate each power term of the M-iUPQC converters that are fundamental active, reactive and apparent power, nonfundamental power and total apparent power. This methodology makes easy the understating of the effect of variation in each variable in the power flow in this conditioner.

The polarities of voltages and currents are shown in Fig. 1.

### B. Fundamental power terms

Firstly, the fundamental power terms of each converter of M-iUPQC were calculated. To calculate the power in each converter, the amplitudes and angles of fundamental terms of current and voltage of srAPF and shAPF needed to be obtained.

Firstly, the fundamental power terms of each converter of M-iUPQC were calculated. To calculate the power in each converter, the amplitudes and angles of fundamental terms of current and voltage of srAPF and shAPF needed to be obtained.

The current of srAPF ( $i_{sr,d}$  in Fig. 1) of M-iUPQC was considered equal to PCC current ( $i_{1pc}$  in Fig.1) because the capacitor  $C_{sr}$  is designed as a high-pass filter and, for grid frequency scale, this capacitor has a high impedance. Thereby, the amplitude of fundamental term of srAPF current can be obtained in function of microgrid active power, the fundamental term of PCC voltage and the angle  $\theta$ .

The amplitude and angle of srAPF voltage can be obtained by the difference between the fundamental term of PCC and the microgrid voltage.

To obtain the amplitude and angle of the fundamental term of the shAPF current, the sum of the currents in node 1 was made. Lastly, the amplitude and angle of shAPF voltage are the microgrid voltage itself.

The fundamental power terms equations are given by (1) to (6).

$$P_{1srX}(\theta, \delta) = \frac{P_{ulT}}{V_{1pcT} \cdot \cos(\theta)} \cdot (V_{1pcX} \cdot \cos(\theta) - V_{1ul} \cdot \cos(\theta - \delta)) \quad (1)$$

$$Q_{1srX}(\theta, \delta) = \frac{P_{ulT}}{V_{1pcT} \cdot \cos(\theta)} \cdot (V_{1ul} \sin(\theta - \delta) - V_{1pcX} \sin(\theta)) \quad (2)$$

$$S_{1srX}(\theta, \delta) = \sqrt{P_{1srX}(\theta, \delta)^2 + Q_{1srX}(\theta, \delta)^2} \quad (3)$$

$$P_{1shX}(\theta, \delta) = \frac{P_{ulT} \cdot V_{1ul} \cdot \cos(\theta - \delta)}{V_{1pcT} \cdot \cos(\theta)} - V_{1ul} \cdot I_{1ulX} \cos(\varphi_{ulX}) \quad (4)$$

$$Q_{1shX}(\theta, \delta) = V_{1ul} \cdot I_{1ulX} \sin(\varphi_{ulX}) - \frac{P_{ulT} \cdot V_{1ul} \sin(\theta - \delta)}{V_{1pcT} \cdot \cos(\theta)} \quad (5)$$

$$S_{1shX}(\theta, \delta) = \sqrt{P_{1shX}(\theta, \delta)^2 + Q_{1shX}(\theta, \delta)^2} \quad (6)$$

Where suffix X indicates the respective phase,  $P_{ulT}$  is the total active power of the microgrid loads,  $V_{1pcX}$  is the fundamental PCC voltage in the respective phase,  $V_{1pcT}$  is sum of the amplitudes of the fundamental PCC voltages in phases A, B and C,  $V_{1ul}$  is the amplitude of microgrid voltage,  $I_{1ulX}$  and  $\varphi_{ulX}$  are the amplitude and angle of fundamental term of microgrid load current in the respective phase where  $\varphi_{ulX}$  is the difference of the angle of microgrid voltage and current.

### C. Nonfundamental and total power terms

In the M-iUPQC, the srAPF current and microgrid voltage, ideally, do not have harmonic distortion. Besides that, the nonfundamental terms of microgrid load currents are compensated by shAPF. Therefore, the nonfundamental power term of shAPF ( $S_{Nsh}$ ) is given by (7).

$$S_{Nsh}(\theta, \delta) = V_{1ulX} \cdot I_{1ulX} \cdot THD_{iulX} \quad (7)$$

Where  $THD_{iulX}$  is total harmonic distortion of the current in the respective phase.

The nonfundamental power of srAPF ( $S_{Nsr}$ ) is shown in (8) and is given by the product of nonfundamental PCC voltage and srAPF current.

$$S_{Nsr}(\theta, \delta) = V_{1ulX} \cdot THD_{vpcX} \cdot \frac{P_{ulr}}{V_{1pcT} \cdot \cos(\theta)} \quad (8)$$

Where  $THD_{vpcX}$  is total harmonic distortion of the PCC voltage in the respective phase.

Finally, (9) and (10) give the total apparent power srAPF ( $S_{sr}$ ) and shAPF ( $S_{sh}$ )

$$S_{sr}(\theta, \delta) = \sqrt{S_{1sr}(\theta, \delta)^2 + S_{Nsr}(\theta, \delta)^2} \quad (9)$$

$$S_{sh}(\theta, \delta) = \sqrt{S_{1sh}(\theta, \delta)^2 + S_{Nsh}(\theta, \delta)^2} \quad (10)$$

With these equations, it is possible to evaluate the power flow of each phase in the iUPQC-M STACOM using PAC.

### III. SIMULATIONS AND EQUATIONS VALIDATION

To validate the previous mathematical analysis, numerical simulations using the software PSIM 9.0 were performed. The simulated system consists of an M-iUPQC operating as a microgrid interface converter, as shown in Figure 1, where the grid is providing active power to the microgrid loads. The design of the power elements and control strategy of the conditioner was made as is presented in [9]. The microgrid was modeled as a load set composed by a linear RL, a three-phase rectifier with capacitive filter and a RL load supplied by a single-phase full-wave rectifier. A balanced loads and PCC voltages scenarios were evaluated.

The simulations were performed using the following specifications:

- Nominal apparent power of iUPQC: 2.5 kVA.
- Microgrid bus line voltage: 220 V.
- Fundamental PCC line voltage: 220 V.
- PCC voltage total harmonic distortion (THD): 11.6%.
- Total apparent power of microgrid loads: 1.71 kVA.
- Fundamental apparent power of microgrid loads: 1.68 kVA.
- Fundamental power factor of microgrid: 0.89, lag.
- THD of microgrid load current: 20%.

The PCC voltage and microgrid current signals is shown in Fig. 2. The simulations were performed varying  $\theta$  and  $\delta$  angles in a range of  $0^\circ$ ,  $\pm 20^\circ$  and  $40^\circ$ . The single phase calculated and simulated results of fundamental active, reactive and apparent power terms of srAPF shared and shAPF are shown in Fig3(a) to Fig. 3(e), respectively, where the marked points are the simulated results and the line graphs are the calculated results. As are shown in Fig. 3, the simulated and calculated results of fundamental terms converged to the same values for all simulations performed, validating the equations obtained in this analysis.

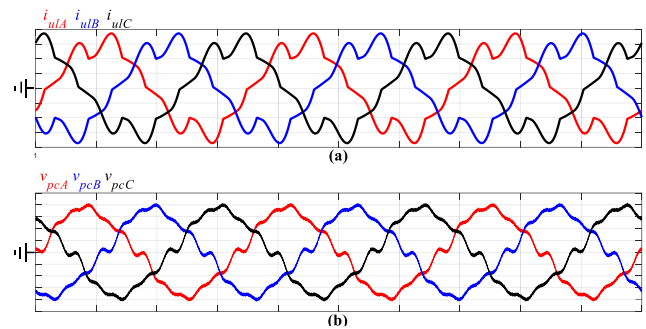


Fig. 2. (a) Microgrid load current (2 A/div, 10 ms/div) and (b) PCC voltage (50 V/div and 10 ms/div) signal of balanced scenario.

Besides that, with  $\theta \in \delta$  in  $0^\circ$ , the reactive power of srAPF (Fig. 3(b)) is around zero while the reactive power of shAPF (Fig. 3(e)) is equal to the reactive power of microgrid loads. It is caused because the fundamental PCC voltage is equal to the load voltage and there is no voltage across srAPF transformer. Consequently, there is not power in srAPF. However, in the M-iUPQC, all current from grid to microgrid side flow by srAPF. For this reason, srAPF has power losses in function of the current however it does not compensate the load disturbances. Keeping  $\delta$  equal to  $0^\circ$  and for positive  $\theta$  angles, iUPQC is providing reactive power to the grid. However, the srAPF voltage is kept in 0 V and the shAPF needs to supply the reactive for grid and load, increasing shAPF power as previously stated. It increases the unbalanced power compensated by each converter.

Changing the angle  $\delta$ , a voltage across srAPF transformer is imposed. Consequently, the srAPF starts to have power processing. For positive  $\delta$  angle, srAPF also supply reactive power then shAPF supply less power, decreasing the power that shAPF need to compensate. Even though, for  $\delta$  different of  $0^\circ$ , active power circulates between srAPF and shAPF (Fig. 3(a) and Fig. 3(d)), the fundamental apparent power, of shAPF decreases considerably, as show in Fig. 3(c) and 3(f). For this reason, PAC is efficient to balance the power compensate by each converter and for optimizing iUPQC, compensating more power with the same hardware, increases the efficiency because the current in shAPF reduces and make modular projects easier as soon as the power processed by each converter can be balanced. For the nonfundamental power terms of srAPF and shAPF, as shown in Fig. 4(a) and Fig. 4(b), respectively, there is a small difference between simulated and calculated results. It is caused by the harmonics of current and voltage in the switching frequency, which was not considered in the equations developed. Anyway, this noted difference did not affect significantly total apparent power of srAPF and shAPF, as are shown Fig. 4(c) and Fig. 4(d), respectively.

Besides that, the  $\delta$  variation does not imply in nonfundamental power sharing between the srAPF and shAPF. The srAPF compensates all the harmonic terms of PCC voltage and the shAPF, compensates all harmonic terms of load current. It means that using PAC is not possible to share the power nonfundamental power terms between the converters of iUPQC. In applications where the load harmonic content be very high, the PAC technique may be not much useful to balance the power of iUPQC converters. Anyway, in this scenario and considering the advantages of balance the powers of iUPQC converters, the PAC technique can be applied to balance the power between the converters of iUPQC.

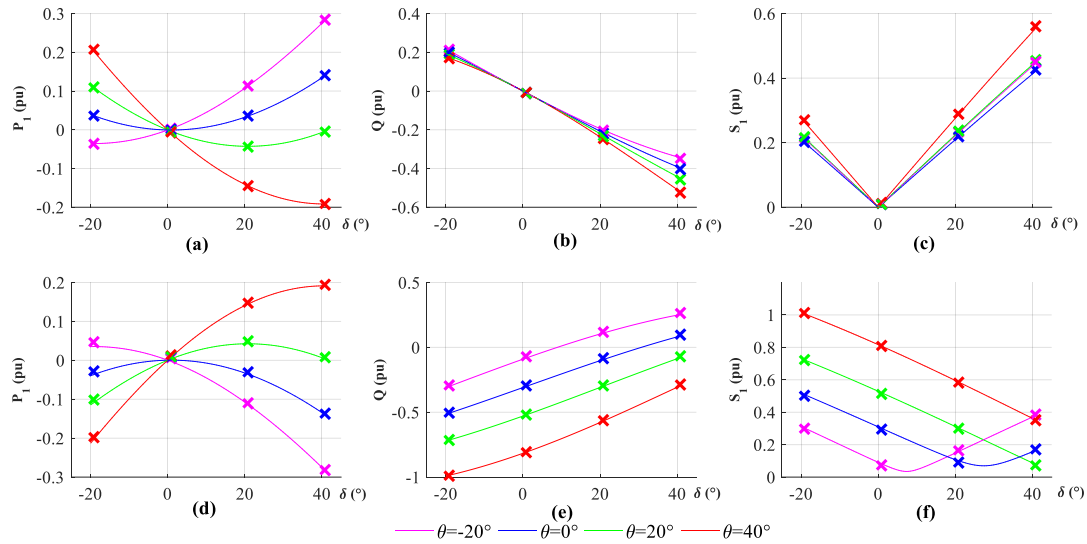


Fig. 3. Calculated and simulated results of fundamental terms in balanced scenario. (a) fundamental term of active power of srAPF, (b) fundamental term of reactive power of srAPF, (c) fundamental term of apparent power of srAPF, (d) fundamental term of active power of shAPF, (e) fundamental term of reactive power of shAPF, (f) fundamental term of apparent power of shAPF.

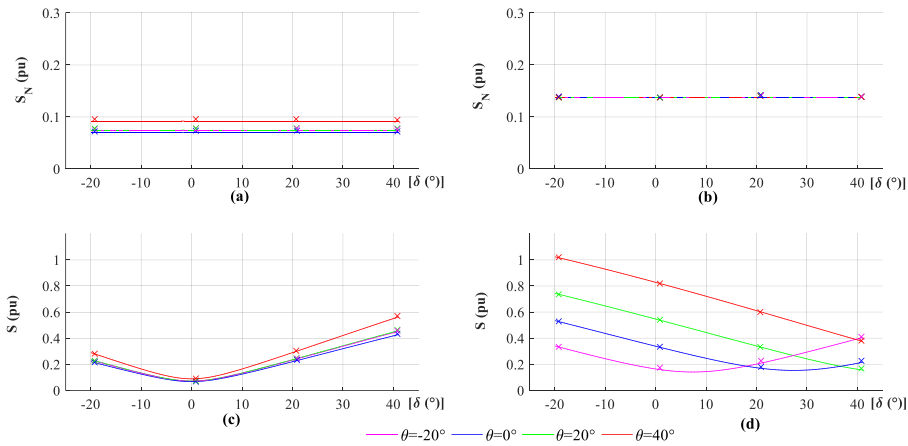


Fig. 4. Calculated and simulated results of nonfundamental and total apparent power terms of balanced scenario. (a) nonfundamental power term of srAPF, (b) nonfundamental power term of shAPF, (c) total apparent power of srAPF, (d) total apparent power of shAPF.

#### IV. POWER ANGLE CONTROL SCHEME

In this Section, a PAC scheme is proposed and validated by numerical simulations.

##### A. PAC scheme proposed

The main goal of the PAC in this paper is to balance the power processed by each converter of M-iUPQC to optimize the power available in this converter for a wide range of applications, to allow the modularity of the converter and to improve the efficiency of the converter.

To achieve this goal, in this paper is proposed an algorithm that use the difference between the 3-phase average of the total apparent power of shAPF and srAPF to define a  $\delta$  angle step. As demonstrated in the Section III, in the proposed scenario, if the total apparent power processed by shAPF is bigger than in the srAPF, the angle  $\delta$  should be increased. Otherwise, the  $\delta$  angle should be decreased. Therefore, it was defined that the PAC algorithm will compare the power difference between shAPF and srAPF and will increment the  $\delta$  when the power in shAPF be bigger than srAPF and the vice versa. The  $\delta$  increment was defined as  $1^\circ$ , to minimize the shAPF voltage perturbation.

Besides that, even a small change in the  $\delta$  angle will cause a perturbation in the microgrid and grid bus voltage because the shAPF control voltage reference receives a step in the voltage. To minimize this issue, it was defined a maximum and minimum power difference target value ( $tg_{max}$  and  $tg_{min}$ ) where are 0.1 and 0.05 pu, respectively. The algorithm starts with the  $tg_{max}$ . If the power unbalanced be bigger than  $tg_{max}$ , the  $\delta$  will be changed and target is set to  $tg_{min}$  until the power unbalanced be smaller than this value. If the target be smaller than  $tg_{min}$ , the target is set to  $tg_{max}$  again. This is done to ensure that the power unbalance will be in the middle of  $tg_{max}$  range, avoiding that the  $\delta$  stayed in the top or the bottom of  $tg_{max}$  range, reducing  $\delta$  variations.

Finally, in the Section III was demonstrated that for bigger positive  $\delta$  angles, an active power circulation between the converters of M-iUPQC occurs. Therefore, the  $\delta$  range was defined to be limited in a range of  $\pm 50^\circ$ . Besides that, to minimize this active power circulation, it was defined that the power in the shAPF should be bigger than in srAPF to allow a smaller  $\delta$  angle and active power circulation between the converters of M-iUPQC.

Therefore, an algorithm to balance the power of the M-iUPQC converter was developed as shown in the flowchart of the Fig. 5

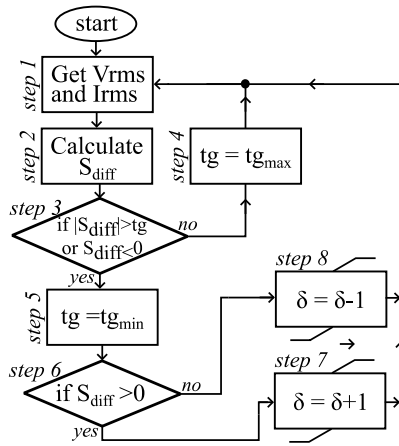


Fig. 5: Flowchart of the proposed PAC scheme.

The algorithm starts with  $\delta$  in  $0^\circ$  and the target ( $tg$ ) set to the maximum value ( $tg_{max}$ ). In the step 1, the RMS voltage and current of srAPF and shAPF is measured. In the step 2, the total apparent power of srAPF and shAPF is calculated by the voltage and current multiplication of the respective converter. Then, the difference of the power between shAPF and srAPF ( $S_{diff}$ ) is calculated as shown in (11).

$$S_{diff} = S_{sh} - S_{sr} \quad (11)$$

In the step 3, the algorithm check if the absolute value of  $S_{diff}$  is bigger than the target value or if the power in srAPF is bigger than in shAPF ( $S_{diff} < 0$ ). If yes, the target is set to  $tg_{min}$  (step 5) and the  $\delta$  angle is changed according to the power unbalance (steps 6, 7 and 8) and the process comes back to step 1. If not, the target value is set to  $tg_{max}$  and the process returns to step 1.

In the steps 7 and 8, the absolute value of delta is limited to  $\pm 50^\circ$ , as previously stated.

The RMS voltage and current measurements was implemented in a way that the value is updated each grid cycle. Therefore, the frequency of the flowchart shown in the Fig. 5 is limited to the half of the grid frequency.

### B. PAC scheme simulation

To validate the proposed PAC scheme, a numerical simulation was performed. The simulation was made using the software PSIM 9.0 and the PAC algorithm was implemented

using the tool C block, that allow the implementation of a software using C language.

The simulated system consists of an M-iUPQC operating as a microgrid interface converter, as was done in the Section III of this paper.

The simulation started with the microgrid loads and PcC voltage as specified in the Section III of this paper, angles  $\theta$  and  $\delta$  in  $0^\circ$ , RMS and PAC disable. In the instant t1, PAC is enable. In t2, after 600 ms, the  $\theta$  is set to  $30^\circ$ . In t3, after 600 ms, a RL load of 0.625 pu and a fundamental power factor of 0.6 is connected to each microgrid phase. Finally, in t4, the RL load connected in t3 is disconnected. The simulation results are shown Fig. 6, where the red and blue lines are the RMS PAC and RMS microgrid current, respectively. The green line is the  $\delta$  angle. Finally, black and purple lines are respectively the total apparent power of shAPF and srAPF, respectively.

As are shown in the Fig. 6, the PAC scheme proposed was efficient to balance the power processed by each converter of M-iUPQC because the total apparent power of the M-iUPQC converters were balanced for all conditions. Besides that, the control scheme is stable and the  $\delta$  angle was changed only a significant power change happens. If PAC was not enabled in this scenario, the power processed by shAPF would be bigger than its rated power that could damage the converter or forcing a failure in the system to protect the converter.

Therefore, with the PAC scheme proposed, the power available in the converters is optimized allowing the converter to process more power for a wide range of scenarios.

### V. CONCLUSIONS

In this paper, the power flow in the M-iUPQC using PAC was evaluated through analytical and numerical simulation. The simulations were performed in balanced scenario to simplify this analysis. Besides that, a PAC scheme was proposed and validated by numerical simulations.

It was demonstrated that PAC is efficient in the control and balance of the power processed by each converter of M-iUPQC even with the variation of  $\theta$  angle and in a scenario of balance microgrid loads and PAC voltage. In addition, with the balancing of the power process by each converter, it was demonstrated that in the scenario evaluated the total power that a MS-iUPQC can process increases because the use of srAPF is optimized, reducing the power processed by shAPF. This feature is important to allow iUPQC to provide more

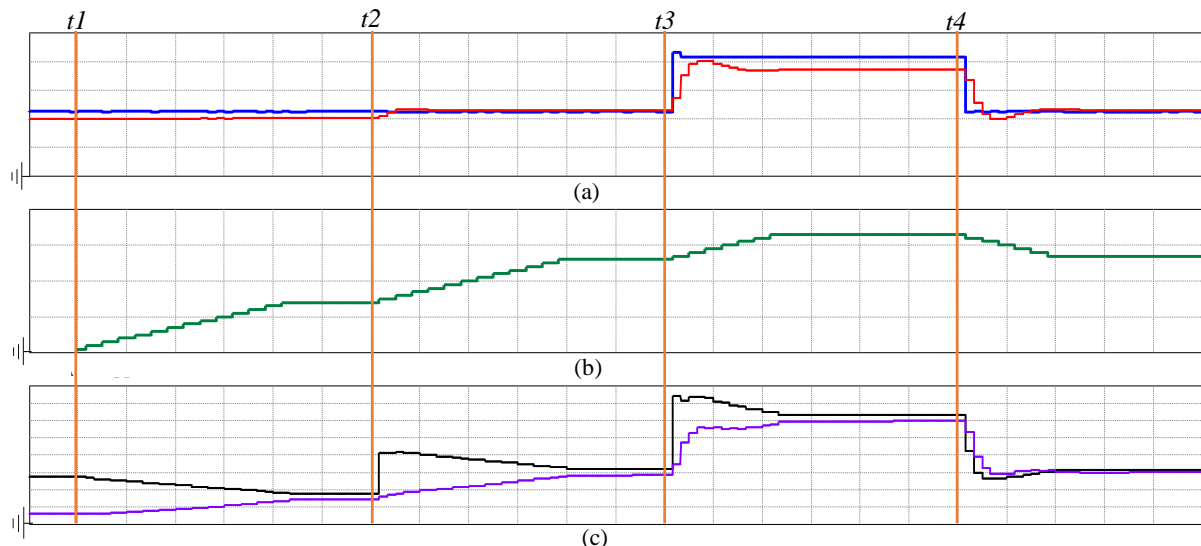


Fig. 6: Simulated results with PAC scheme enabled. (a) RMS current of PCC (red) and microgrid (blue) (2 A/div); (b)  $\delta$  angle (green) (10%/div); (c) total apparent power of shAPF (black) and srAPF (purple) (100 VA/div). Time axis scale: 100 ms/div.

power reactive power to grid when it is operating as STATCOM.

For next steps and future studies, the authors are considering the study of the power flow and the improvement of PAC scheme proposed for an unbalanced scenario, if necessary.

#### REFERENCES

- [1] M. H. Saeed, W. Fangzong, B. A. Kalwar and S. Iqbal, "A Review on Microgrids' Challenges & Perspectives," in *IEEE Access*, vol. 9, pp. 166502-166517, 2021, doi: 10.1109/ACCESS.2021.3135083.
- [2] N. Rezaei and M. N. Uddin, "An Analytical Review on State-of-the-Art Microgrid Protective Relaying and Coordination Techniques," in *IEEE Transactions on Industry Applications*, vol. 57, no. 3, pp. 2258-2273, May-June 2021, doi: 10.1109/TIA.2021.3057308.
- [3] E. Espina, J. Llanos, C. Burgos-Mellado, R. Cárdenas-Dobson, M. Martínez-Gómez and D. Sáez, "Distributed Control Strategies for Microgrids: An Overview," in *IEEE Access*, vol. 8, pp. 193412-193448, 2020, doi: 10.1109/ACCESS.2020.3032378.
- [4] Shubhra and B. Singh, "Solar PV Generation Based Microgrid Control Interfaced to Utility Grid," *2020 21st National Power Systems Conference (NPSC)*, 2020, pp. 1-6, doi: 10.1109/NPSC49263.2020.9331928.
- [5] P. Tenti, T. Caldognetto, S. Buso and A. Costabeber, "Control of utility interfaces in low voltage microgrids," *2014 IEEE 5th International Symposium on Power Electronics for Distributed Generation Systems (PEDG)*, 2014, pp. 1-8, doi: 10.1109/PEDG.2014.6878674.
- [6] A. A. P. Machado, D. I. Brandao, I. A. Pires and B. d. J. C. Filho, "Fault-tolerant Utility Interface power converter for low-voltage microgrids," *2017 IEEE 8th International Symposium on Power Electronics for Distributed Generation Systems (PEDG)*, 2017, pp. 1-5, doi: 10.1109/PEDG.2017.7972469.
- [7] I. Khan, A. S. Vijay and S. Doolla, "Nonlinear Load Harmonic Mitigation Strategies in Microgrids: State of the Art," in *IEEE Systems Journal*, doi: 10.1109/JSYST.2021.3130612.
- [8] M. Aredes and R. M. Fernandes, "A dual topology of Unified Power Quality Conditioner: The iUPQC," *2009 13th European Conference on Power Electronics and Applications*, 2009, pp. 1-10.
- [9] R. J. Millnitz dos Santos, J. C. da Cunha and M. Mezaroba, "A Simplified Control Technique for a Dual Unified Power Quality Conditioner," in *IEEE Transactions on Industrial Electronics*, vol. 61, no. 11, pp. 5851-5860, Nov. 2014, doi: 10.1109/TIE.2014.2314055.
- [10] S. Paithankar and R. Zende, "Comparison between UPQC, iUPQC and improved iUPQC," *2017 Third International Conference on Sensing, Signal Processing and Security (ICSSS)*, 2017, pp. 61-64, doi: 10.1109/SSPS.2017.8071565.
- [11] B. W. França, L. F. da Silva, M. A. Aredes and M. Aredes, "An Improved iUPQC Controller to Provide Additional Grid-Voltage Regulation as a STATCOM," in *IEEE Transactions on Industrial Electronics*, vol. 62, no. 3, pp. 1345-1352, March 2015, doi: 10.1109/TIE.2014.2345328.
- [12] S.M. Fagundes, F.L. Cardoso, E.V. Stangler, F.A.S. Neves, M. Mezaroba, A detailed power flow analysis of the dual unified power quality conditioner (iUPQC) using power angle control (PAC), in *Electric Power Systems Research*, vol. 192, 2021, 106933, ISSN 0378-7796, doi: 10.1016/j.epsr.2020.106933
- [13] S. M. Fagundes and M. Mezaroba, "Reactive power flow control of a Dual Unified Power Quality Conditioner," *IECON 2016 - 42nd Annual Conference of the IEEE Industrial Electronics Society*, 2016, pp. 1156-1161, doi: 10.1109/IECON.2016.7793770.
- [14] "IEEE Standard Definitions for the Measurement of Electric Power Quantities Under Sinusoidal, Nonsinusoidal, Balanced, or Unbalanced Conditions," in *IEEE Std 1459-2010 (Revision of IEEE Std 1459-2000)*, vol., no., pp.1-50, 19 March 2010, doi: 10.1109/IEEESTD.2010.5439063.